Catalysis Science & Technology

Accepted Manuscript

ROYAL SOCIETY OF CHEMISTRY

www.rsc.org/catalysis

Journal Name

RSCPublishing

ARTICLE

Highly active three-way catalysis of rhodium particles on a Y-stabilized La-containing ZrO_2 support: Effect of Y on the enhanced reducibility of rhodium and self-regeneration

Hisaya Kawabata,*[ab] Yuki Koda,[a] Hirosuke Sumida,[a] Masahiko Shigetsu,[a] Akihide Takami[a] and Kei Inumaru[b]

Cite this: DOI: 10.1039/x0xx00000x

Received ooth January 2012,
Accepted ooth January 2012

DOI: 10.1039/x0xx00000x

www.rsc.org/

A novel, highly active three-way catalyst, rhodium supported on Y- and La-added zirconia (Rh/Zr–Y–La–O) was found in this study. Rh/Zr–Y–La–O showed superior performance compared with a previously reported Rh on La-added ZrO_2 (Rh/Zr–La–O) catalyst (Kawabata *et al.*, *Chem. Commun.* 2013, 49 (38), 4015; *Catal. Sci. Technol.*, 2014, 4 (3), 697). The effects of Y addition to ZrO_2–based supports were investigated in detail. CO temperature programmed reduction and *in situ* Fourier transform infrared spectra of adsorbed NO species indicated that Y addition to La–containing ZrO_2 enhanced the reducibility of rhodium supported on the catalyst and more metallic Rh was exposed on the surface after oxidation for Rh/Zr–Y–La–O than for Rh/Zr–La–O. Before and after an aging treatment at 1273 K that simulated 80000 km travelled by vehicles, Rh/Zr–Y–La–O showed high steam reforming activity. After the aging treatment, Rh/Zr–Y–La–O was deactivated using an oxidation treatment, but its three-way catalysis activity was completely regenerated after a short (5 min) exposure to steam reforming reaction conditions, demonstrating self-regeneration capability. After the aging treatment, Rh/Zr–Y–La–O showed higher rhodium dispersion than other catalysts. This was attributed to the high surface area of the support after aging and the stabilization of ZrO_2 from the addition of Y. Our findings highlight the role of catalyst supports in designing effective three-way catalysts with high tolerance to the oxidative conditions in new vehicles and engines.

1. Introduction

Three-way catalysis for automotive exhaust purification is an important process that has been extensively studied for several decades.[1-11] Since emission regulations are constantly becoming more stringent worldwide,[12, 13] there has been consistent focus on improving three-way catalytic activity and durability. The conditions to which a catalyst is subjected in automotive exhaust are severe: the temperatures and gas phase compositions quickly change over wide ranges. The most influential condition impeding catalytic activity is atmospheric changes in oxidant and reductant concentrations. Recently, a new type of engine operation was commercialized to minimize fuel consumption; the engine automatically switches off when the car stops for a short time. This new operation causes highly transient and fluctuating conditions, including high oxygen concentrations that deactivate three-way catalysts. Tolerance against oxidative conditions is crucial for designing a highly efficient three-way catalyst for practical applications.[2]

Rhodium is a key catalytic component in three-way catalysts for the effective conversion of CO, hydrocarbons and NO_x to H_2O, CO_2 and N_2.[10, 14] However, rhodium has a number of drawbacks under oxidative conditions.[3, 4] In the case of alumina supports, rhodium readily reacts with the support to form different phases at high temperatures. Rhodium is known to form oxides with various oxidation states, structures and morphologies (rafts or plate-like structures) on alumina supports.[15, 16] Changes in size, shape and phase induced by rhodium interactions with alumina supports significantly affect the activity of the catalysts.[17, 18] Bond formation between Rh and the support is possible for suppressing the sintering behaviour of rhodium.[19] Zirconia has weaker interactions with rhodium than alumina does, and zirconia-modified alumina was reported to be useful for controlling the activity of rhodium.[20]

Previously, we have demonstrated the high catalytic activity of rhodium supported on La-containing ZrO_2 (Rh/Zr–La–O) for the elimination of NO_x, CO and hydrocarbons, through a three-way catalytic process, from a synthetic automotive exhaust gas.[21, 22] The catalyst showed better performance than other catalysts, especially after oxidative pre-treatment, though the catalyst did not contain oxygen-storage components such as CeO_2. The Rh/Zr–La–O catalyst showed high activity in the steam reforming reaction, even after an aging treatment that mimicked a mileage of 80000 km for real vehicles. Exposure to

steam reforming reaction conditions reduced the oxidized Rh on the Zr–La–O support, refreshing the deactivated catalyst. The state of rhodium was not only affected by interactions between the metal particles and the support, but also by the steam reforming reaction occurring over the catalyst. After the aging treatment, the Rh/Zr–La–O catalyst exhibited rhodium sintering and phase separation of the support, indicating that further work is required to develop more efficient catalysts.

In this study, we prepared a novel, highly active three-way catalyst, Rh supported on yttrium- and lanthanum-added zirconia (Rh/Zr–Y–La–O). We also investigated the effect of yttrium addition to ZrO_2-based supports in detail. Yttrium is a typical stabilizing element for zirconia.[23] The redox properties and dispersion of rhodium, and the crystal structure of the support were significantly affected by the addition of Y. The importance of the steam reforming reaction was also demonstrated for the yttrium-added catalyst Rh/Zr–Y–La–O. These investigations aimed to identify the reason for the excellent three-way catalytic activity of Rh/Zr–Y–La–O.

2. Experimental

2-1. Catalyst preparation

The yttrium-stabilized ZrO_2 was prepared using an ammonia-assisted co-precipitation method where zirconium nitrate $ZrO(NO_3)_2{\cdot}6H_2O$ (60.8 g, > 98 %, Nacalai Tesque) and yttrium nitrate $Y(NO_3)_3{\cdot}6H_2O$ (8.7 g) were dissolved in 200 g of water and an aqueous NH_4OH solution (1 %, Wako Pure Chemical Industries, Ltd., Osaka, Japan) was added to raise the pH (≥ 12). The precipitate was filtered, dried at 423 K for 2 h in air, and then calcined at 773 K for 2 h in air to produce the ZrO_2–Y_2O_3 mixed oxide. The ZrO_2–La_2O_3 and Y-stabilized ZrO_2–La_2O_3 mixed oxides were also prepared using the ammonia-assisted co-precipitation method from $Y(NO_3)_3{\cdot}6H_2O$ and $La(NO_3)_3{\cdot}6H_2O$ (Rare Metallic Co., Ltd., Tokyo, Japan). For the preparation of Y-stabilized ZrO_2–La_2O_3, lanthanum nitrate, yttrium nitrate and zirconium nitrate were dissolved in water before adding an aqueous NH_4OH solution. The concentrations of Y and La were 10 and 5 wt % as oxides, respectively. The Y, La and Y–La mixed oxides were designated as Zr–Y–O, Zr–La–O and Zr–Y–La–O, respectively. The ZrO_2 support (Brunauer–Emmett–Teller (BET), surface area: 52.3 $m^2\ g^{-1}$) was purchased from Kishida Chemical Co., Ltd. (Osaka, Japan). Rhodium (0.33 wt % as rhodium metal) was loaded onto the oxide support by impregnation, using an aqueous solution of $Rh(NO_3)_3{\cdot}H_2O$ (Dai-ichi Kigenso Kogyo, Osaka, Japan). The obtained Rh-loaded oxide supports were dried at 393 K for 12 h in air and subsequently calcined in air at 773 K. For evaluating the three-way catalytic reaction, the Rh-loaded ZrO_2 mixed oxide catalysts were deposited on a cordierite honeycomb. To do this, the Rh-loaded powder catalysts were mixed with distilled water and colloidal zirconia (ZSL-10D, Dai-ichi Kigenso Kogyo, Osaka, Japan) was used for binding the catalyst powder to the cordierite honeycomb. The slurry-coated cordierite honeycomb was dried at 473 K for 2 h in air, then calcined at 773 K for 2 h in air. The amount of catalyst coated on the cordierite honeycomb was 100 g dm^{-3}. The resulting products were termed "fresh" catalysts.

2-2. Three-way catalytic reactions

The activity of the Rh-based catalysts was evaluated using a fixed-bed continuous flow reactor. The reaction gas was a mixture of 500 ppm C_3H_6, 1000 ppm NO, 0.7 % CO, 0.2 % H_2, 0.6 % O_2, 13.6 % CO_2 and 10 % H_2O. Nitrogen was used as a diluent. The gas composition mimicked the actual exhaust gas emitted at ≈3000 rpm engine operation. The flow rate of the reaction gas was 26 $dm^3\ min^{-1}$, corresponding to an hourly gas space velocity of 60000 h^{-1}. Prior to catalytic performance measurements, the catalysts were pre-treated under a flow of the gas mixture at 773 K for 10 min and then cooled to 373 K under a flow of nitrogen. The three-way catalytic activity was evaluated over a range of temperatures from 373–773 K (at a heating rate of 30 K min^{-1}). The products were monitored using a flame ionization detector for hydrocarbons, infrared absorption for CO and chemical luminescence for NO using a Horiba MEXA-9100 system (Kyoto, Japan).

2-3. Aging procedure

Accelerated durability tests, or aging treatments, were conducted by treating the fresh catalysts at 1273 K for 24 h in a 2 % O_2 and 10 % H_2O atmosphere (diluent: N_2). This aging treatment simulated empirically a 80000 km of mileage for real vehicles.

2-4. Steam-reforming reaction

The reaction gas was a mixture of 660 ppm C_3H_6 and 2 % H_2O (molar ratio of H_2O/C=10). Nitrogen was used as a diluent. The flow rate of the steam-reforming reaction gas was 26 $dm^3\ min^{-1}$ that corresponds to an hourly gas space velocity of 60000 h^{-1}. The activity of the steam-reforming reaction was measured using a fixed-bed continuous flow reactor the same as three-way catalytic activity measurements. Prior to the activity evaluations, the catalyst was pre-treated under three-way catalytic reaction gas at 773 K for 10 min and then cooled to 373 K under a flow of nitrogen.

2-5. Characterization

For each of the characterization techniques described in sections 2.5.1–2.5.5, catalysts were used in powder form without the cordierite honeycomb.

2-5-1. X-ray diffraction (XRD)

Powder XRD patterns were measured using a RINT-2000 (Rigaku Corporation, Tokyo, Japan) with monochromated Cu Kα radiation (λ = 1.54056 Å). Crystalline phases were identified using PDF files. The mean Rh crystal size was determined from the Rh (111) diffraction peak at 2θ = 40.1° using Scherrer's equation.

2-5-2. Transmission electron microscopy (TEM)

TEM images were taken with a JEM-3000F microscope (JEOL Ltd., Tokyo, Japan). To image the catalyst after the catalytic reaction, the samples were treated under the reaction gas at 773 K for 10 min followed by cooling to room temperature under a nitrogen flow prior to specimen preparation. The range of Rh particle sizes were evaluated from TEM images by counting about 10 to 20 particles from each sample.

2-5-3. Temperature-programmed reduction using CO (CO-TPR)

CO-TPR was carried out using CO (0.6 %) / He as the reductant gas (100 cm^3 min^{-1}) at a heating rate of 30 K min^{-1}. Prior to the TPR measurements, samples were pre-treated under a flow of 5 % O_2 at 773 K for 10 min and then cooled to 323 K under a flow of He. The O/Rh ratios were calculated from the amount of CO_2 formed during TPR. The supports without rhodium were also measured and the amount of evolved carbon dioxide was subtracted from the data of the rhodium-containing catalysts to estimate the rhodium oxidation state using the following equation 1.

$$3CO + Rh_2O_3 \rightarrow 3CO_2 + 2Rh \quad (1)$$

2-5-4. *In situ* Fourier transform infrared (FT-IR) spectra

FT-IR spectra were recorded using a BioRad FTS-155 equipped with a diffuse reflectance *in situ* cell (ST Japan Inc., Tokyo, Japan). To clarify the state of rhodium after oxidation, spectra of adsorbed NO were measured. The sample was first pre-treated in 5 % O_2 in He at 773 K for 10 min and then cooled to 373 K under a flow of He. First, background spectra were taken at increasing temperatures from 373–773 K, with steps of 100 K in a flow of He. Then, the sample was cooled to 373 K under a flow of He and then the flow gas was switched to NO (1000 ppm) / He for each measurement. Spectra were recorded with a resolution of 4 cm^{-1} at each increasing temperature from 373–773 K, with 100 K steps after exposure for 5 min to the gas flow containing the probed molecules for each measurement.

2-5-5. Other characterization techniques

Rhodium dispersion was measured using the CO pulse chemisorption method at 300 K. The catalysts were pre-treated as follows: the catalysts were first heated (heating rate of 30 K min^{-1}) in a flow of O_2 to 573 K and the temperature was held for 10 min. The catalyst temperature was then increased to 673 K in a H_2 flow and the temperature was maintained for 10 min, followed by cooling to 300 K in a He flow. Pulses of known amounts of CO were injected into the flowing gas and the CO concentrations at the outlet of the reactor were monitored using a thermal conductivity detector. The dispersion was calculated from the CO uptake, assuming that CO adsorbed to the surface of the Rh particles with a 1:1 stoichiometry for CO:surface Rh.[30] The rhodium particle size was estimated using the dispersion value from Equation 2, [31]

$$L = f \times M / (\rho \times N_A \times \pi \times r^2 \times D) \quad (2)$$

where L is the particle size (nm), f is the shape factor (spherical = 6), M is the atomic weight (103), ρ is the density (12.4 g cm^{-3}), N_A is Avogadro's number (6.02×10^{23} mol^{-1}), r is the atomic radius (1.34×10^{-10} m) and D is the dispersion. The specific surface areas of the catalysts were measured by the BET one-point method using a Shimadzu Micrometrics Flowsorb 2300, SHIMADZU Corporation, Kyoto, Japan).

3. Results

3-1. Crystal phases of supports

Structural alterations caused by the introduction of Y and La into ZrO_2 were studied using XRD, as shown in Fig. 1. For fresh Rh/ZrO_2, only the monoclinic ZrO_2 phase was detected (Fig. 1a). The addition of either Y or La to ZrO_2 stabilized the high temperature ZrO_2 phases; the cubic ZrO_2 phase was formed for Rh/Zr–Y–O (Fig. 1c), and the tetragonal ZrO_2 phase was formed for Rh/Zr–La–O (Fig. 1e). When both Y and La were added to ZrO_2, the structure became cubic ZrO_2. Regardless of the presence of La, addition of Y into zirconia caused the formation of the cubic phase (Fig. 1c and g). No diffraction peak of Rh was detectable for the fresh catalysts.
After the aging treatment at 1273 K, the structure of Rh/ZrO_2 did not change from monoclinic ZrO_2 (Fig. 1b). For Rh/Zr–La–O after the aging treatment, the tetragonal ZrO_2 transformed into three phases. One was tetragonal ZrO_2 as the major phase, and the others were monoclinic ZrO_2 and $La_2Zr_2O_7$ as minor phases (Fig. 1f). $La_2Zr_2O_7$ had a pyrochlore structure with 1:1

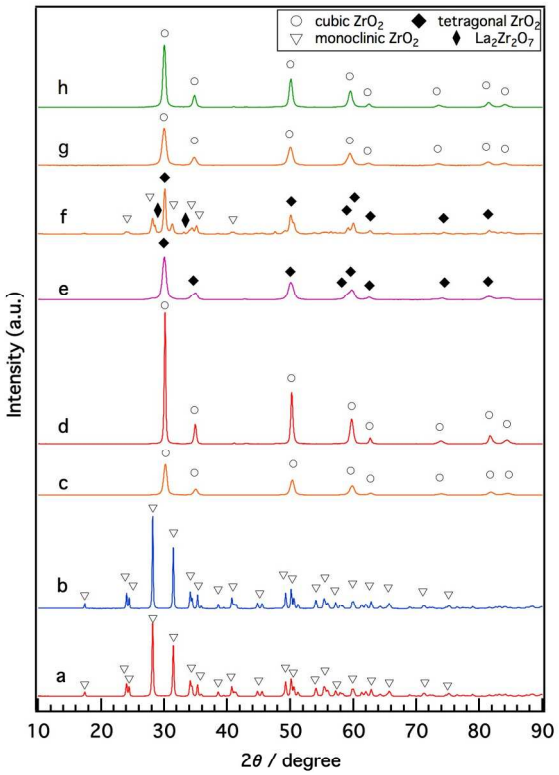

Fig. 1. XRD patterns of (a) fresh Rh/ZrO_2, (b) aged Rh/ZrO_2, (c) fresh Rh/Zr–Y–O, (d) aged Rh/Zr–Y–O, (e) fresh Rh/Zr–La–O, (f) aged Rh/Zr–La–O, (g) fresh Rh/Zr–Y–La–O and (h) aged Rh/Zr–Y–La–O. Aging was conducted at 1273 K in a 2 % O_2, 10 % H_2O, N_2 atmosphere for 24 h.

molar ratio of La and Zr. In contrast, as shown in Fig. 1d and h, the cubic ZrO_2 phase was maintained, even after the aging treatment, for Rh/Zr–Y–O and Rh/Zr–Y–La–O. The introduction of Y to ZrO_2 resulted in the formation of the cubic ZrO_2 phase for both the fresh and aged catalyst. Rhodium diffraction peaks for the aged catalysts were very weak but Rh 111 peak was detectable for some aged catalysts (Fig. S1 in ESI).

3-2. Effects of oxidation treatment on the performance of the three-way rhodium-based catalysts

Because of recently developed engine operations, catalytic activity after exposure to oxidative conditions is an important criterion for applications in real vehicles. We have previously reported that Rh/Zr–La–O showed higher three-way catalytic activity compared with Rh/ZrO_2 and rhodium supported on other lanthanide (Ce, Pr or Nd)-added ZrO_2.[21, 22] In this study, the catalytic activities were evaluated for Y-stabilized ZrO_2 and for Y-stabilized Zr–La–O using two different pre-treatments. The first was a treatment under the reaction gas (simulated automotive exhaust) and the second was under oxidative conditions. For the fresh catalysts, their activities after treatment under the reaction gas and after the oxidation pre-treatment are shown in Figs. 2 and 3, respectively. Figures 4 and 5 present the activities of the aged catalysts after the two different pre-treatments. In each figure, the top panel shows hydrocarbon conversion and the bottom panel shows NO_x conversion. Corresponding CO conversions are also provided in ESI as Figs. S2 to S5.

First, the effects of Y addition on the activity of the fresh catalysts were studied. After the reaction gas pre-treatment, the activity of Rh/Zr–Y–O decreased compared with Rh/ZrO_2 for both hydrocarbon conversion (Fig. 2a) and NO_x conversion (Fig. 2b). For Y addition to the Rh/Zr–La–O, hydrocarbon and NOx conversion were both enhanced, as shown in Fig. 2a and b, respectively. This indicates that Rh/Zr–Y–La–O had higher catalytic activity than the previously reported Rh/Zr–La–O catalyst.

The effects of Y addition on the activities of the fresh catalysts that underwent the oxidative pre-treatment were also investigated. Figure 3 presents the results of the activity tests. After the oxidative pre-treatment, Rh/Zr–Y–O showed almost the same hydrocarbon conversion activity as Rh/ZrO_2 (Fig. 3a) and the activity of Rh/Zr–Y–La–O was comparable to that of Rh/Zr–La–O. For NOx conversion, Y addition slightly enhanced the activity for Rh/Zr–Y–La–O and Rh/Zr–Y–O

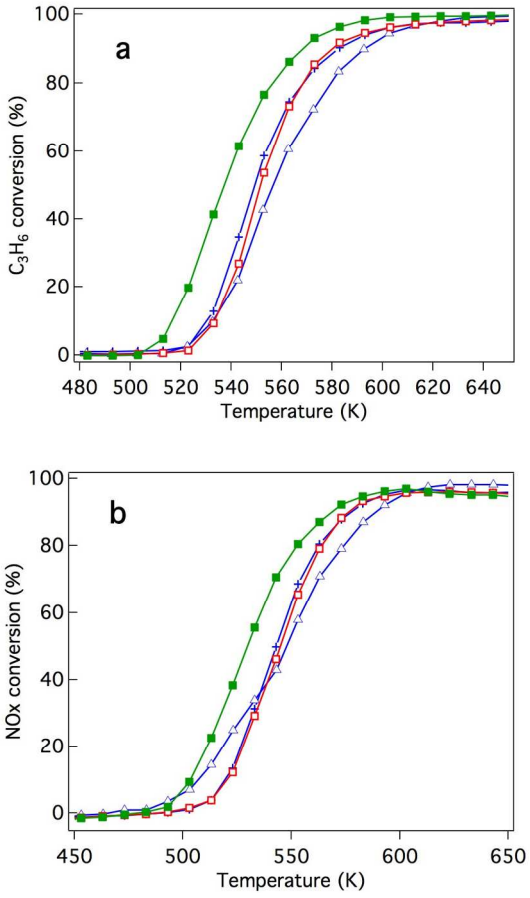

Fig. 2. Conversion of the fresh three-way catalysts that underwent the reaction gas pre-treatment for (a) C_3H_6 conversion and (b) NO conversion. The catalysts studied were (+) Rh/ZrO_2, (△) Rh/Zr–Y–O, (□) Rh/Zr–La–O, and (■) Rh/Zr–Y–La–O.

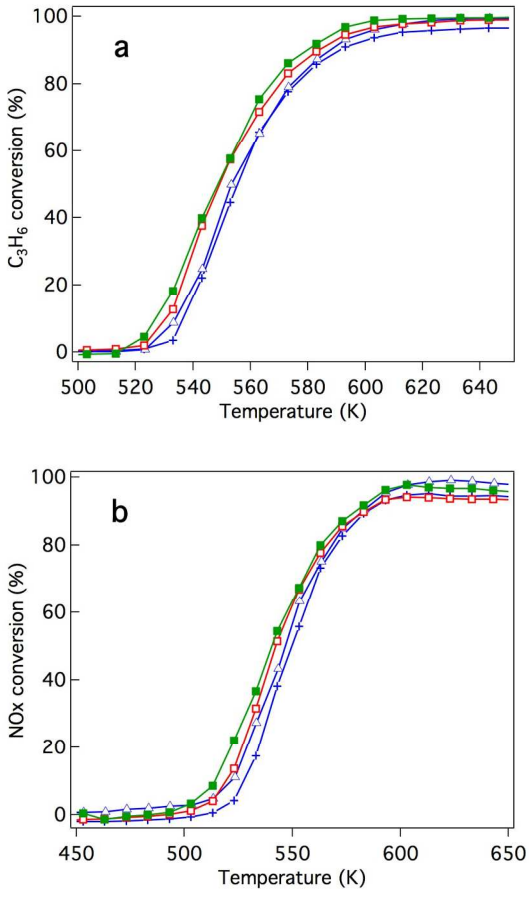

Fig. 3. Conversion by the fresh three-way catalysts that underwent the oxidation treatment for (a) C_3H_6 conversion and (b) NO conversion. The catalysts studied were (+) Rh/ZrO_2, (△) Rh/Zr–Y–O, (□) Rh/Zr–La–O, and (■) Rh/Zr–Y–La–O.

compared with the catalyst without Y (Fig. 3b). Rh/Zr–Y–La–O had the best catalytic activity after the oxidative pre-treatment.

The NO conversion started at 500K, which was lower temperature compared to the C_3H_6 conversion (520K). The conversion of CO started at almost the same temperature as NO conversion (Figs. S2 to S5 of the ESI). NO must have reacted with CO and/or H_2 in the reaction gas before C_3H_6 started to convert.

The effects of Y addition on the activities of the aged catalysts were also studied, as shown in Fig. 4. After the reaction gas pre-treatment, Rh/Zr–Y–O had higher hydrocarbon and NO_x conversion than Rh/ZrO_2. Also, Rh/Zr–Y–La–O had higher hydrocarbon and NO_x conversion than Rh/Zr–La–O (Fig. 4a and b). Among the tested catalysts, Rh/Zr–Y–La–O had the highest activity for hydrocarbon and NO_x conversions. After the oxidative pre-treatment of the aged catalysts (Fig. 5), the activity of Rh/Zr–Y–La–O was comparable to, or slightly lower than, that of Rh/Zr–La–O. Rh/Zr–Y–O also had activities similar to Rh/Zr–Y–La–O. Rh/ZrO_2 had much lower activity than the other catalysts under these conditions.

We measured the inlet and outlet temperatures of the catalyst bed at the working state of three-way catalysis by using thermocouples. When the conversion of C_3H_6 and NO started in three-way catalytic reaction at around 520K, the outlet temperature showed higher values than the inlet temperature (See Fig. S6 in ESI), indicating the occurrence of exothermic reaction (e.g. hydrocarbon oxidation). When the temperature raised up to 673K, however, the outlet temperature became lower than the inlet temperature. This phenomenon demonstrated that the endothermic reaction such as steam-reforming reaction was taking place during the three-way catalysis.

3-3. Rhodium particle sizes and dispersion on different supports

Figure 6 presents TEM images of the catalysts before and after the aging treatment. Figure 6a–d are images of fresh catalysts after the three-way catalytic run at 773 K for Rh/ZrO_2, Rh/Zr–Y–O, Rh/Zr–La–O and Rh/Zr–Y–La–O, respectively. Figure 6e–h are images of the aged catalysts presented in the same order as Fig. 6a–d. The particle size range of the support was 10–20 nm for Zr–Y–O (Fig. 6b), while for ZrO_2 the particle size range was 50–70 nm (Fig. 6a). Particle sizes for the Zr–La–O and Zr–Y–La–O supports both ranged from 10–20 nm (Fig. 6c and d). For the fresh catalysts, the support oxides

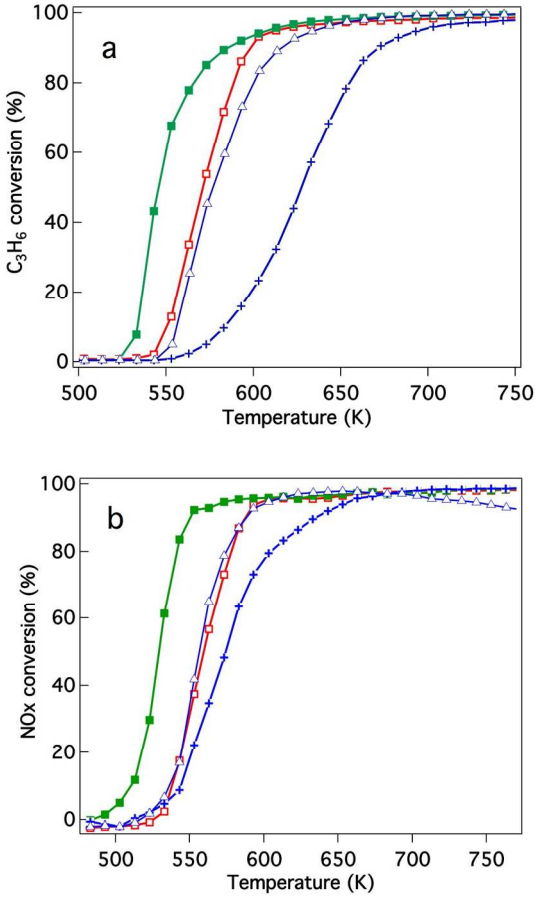

Fig. 4. Conversion by the aged three-way catalysts that underwent the reaction gas pre-treatment for (a) C_3H_6 conversion and (b) NO conversion. The catalysts studied were (+) Rh/ZrO_2, (△) Rh/Zr–Y–O, (□) Rh/Zr–La–O, and (■) Rh/Zr–Y–La–O.

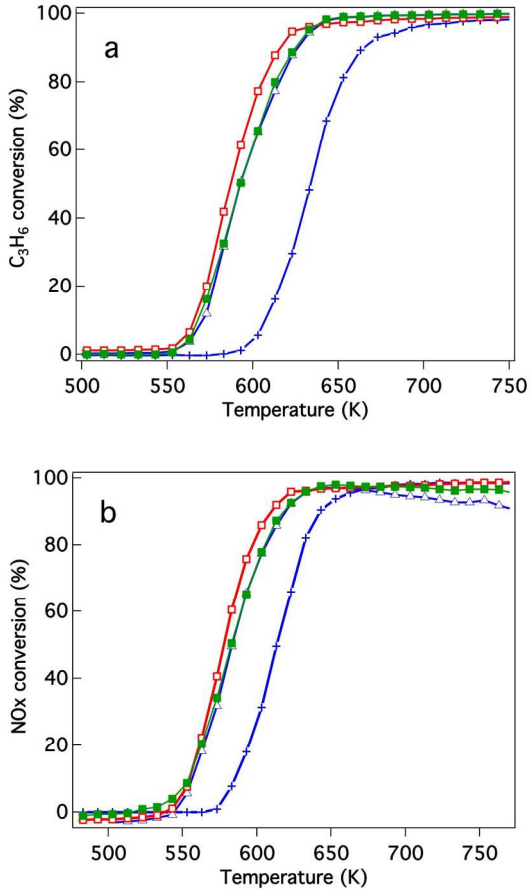

Fig. 5. Conversion by the aged three-way catalysts that underwent the oxidation treatment for (a) C_3H_6 conversion and (b) NO conversion. The catalysts studied were (+) Rh/ZrO_2, (△) Rh/Zr–Y–O, (□) Rh/Zr–La–O, and (■) Rh/Zr–Y–La–O.

formed smaller particles when La or Y was added. After the aging treatment, the particle size ranges for ZrO_2 and Zr–Y–O were 50–100 nm, indicating that the support particles of fresh catalysts sintered to form larger ones during the aging treatment (Fig. 6e and f). Conversely, the particle size ranges for Zr–La–O and Zr–Y–La–O were 10–20 nm, even after the aging treatment, implying that the La-containing supports do not readily sinter. The surface areas of these catalysts were in agreement with their particle sizes (Table 1). The BET surface areas of Rh/ZrO_2 and Rh/Zr–Y–O, in which support particle growth was observed, were 16.4 and 21.4 m^2g^{-1}, respectively. Rh/Zr–La–O and Rh/Zr–Y–La–O, which had smaller particle sizes, had higher surface areas of 29.6 and 51.2 m^2g^{-1}, respectively. The largest surface area was measured for Rh/Zr–Y–La–O, and the decrease in the surface area of this catalyst from the aging treatment was small (from 75.3 m^2g^{-1} to 51.2 m^2g^{-1}) compared with the other catalysts.

The effect of Y addition on rhodium particle size is even more important. The rhodium particle size was approximately 1–2 nm for the fresh catalysts prepared in this study, as shown in Fig. 6a–d (the arrows indicate Rh particles). Table 1 lists the dispersion of Rh estimated by CO adsorption at 300 K for both the fresh and the aged catalysts. Rhodium dispersion in the fresh catalysts was greater than 50 % and Rh particle sizes estimated from the dispersion were approximately 2 nm, being consistent with the TEM observations. Rhodium particle sizes did not appear to be affected by the addition of Y. The presence of rhodium was confirmed from energy-dispersive x-ray (EDX) analysis for all the fresh and aged catalysts. For aged Rh/ZrO_2, spherical rhodium particles with diameters of approximately 10 nm were observed (Fig. 6e). Aged Rh/Zr–Y–O contained larger rhodium particles (diameter = 70 nm), as shown in Fig. 6f (EDX data are given as Fig. S7 in ESI). For aged Rh/Zr–La–O, large rhodium particles (30–100 nm, most likely thin, plate-like particles based on their pale contrasts) were observed (Fig. 6g, EDX data are given as Fig. S8 in ESI). No nano-sized rhodium particles were detected in Rh/Zr–Y–O and Rh/Zr–La–O. In the TEM image of Rh/Zr–Y–La–O (Fig. 6h), a number of small rhodium particles (approximately 5 nm in size) were observed, while the particle size estimated by Scherrer's equation using the Rh 111 diffraction peak (Fig. S1 in ESI) was approximately 80 nm, suggesting that larger particles were present in areas outside that covered in the TEM analysis. Although the Rh dispersion for all of the aged catalysts was quite low (below 10 %), aged Rh/Zr–Y–La–O exhibited the highest dispersion among the aged catalysts tested in this study. The rhodium particle sizes were calculated from the dispersion assuming that the particles were spherical. The values were 22.6, 27.7, 32.6 and 15.8 nm for Rh/ZrO_2, Rh/Zr–Y–O, Rh/Zr–La–O and Rh/Zr–Y–La–O, respectively. The smaller mean rhodium size for Rh/Zr–Y–La–O was consistent with the TEM observations.

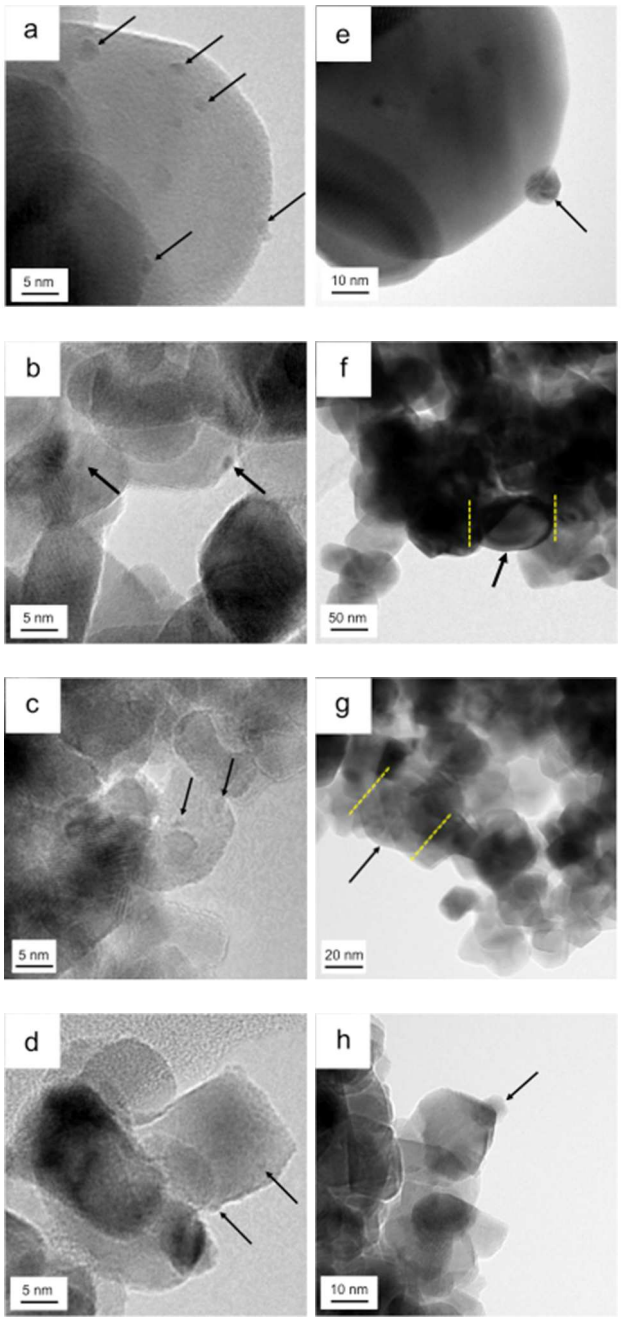

Fig. 6. TEM images of (a) fresh Rh/ZrO_2, (b) fresh Rh/Zr–Y–O, (c) fresh Rh/Zr–La–O, (d) fresh Rh/Zr–Y–La–O, (e) aged Rh/ZrO_2, (f) aged Rh/Zr–Y–O, (g) aged Rh/Zr–La–O, and (h) aged Rh/Zr–Y–La–O. Aging was conducted at 1273 K and in 2 % O_2 and 10 % H_2O/N_2 for 24 h.

Table 1 Measured properties of the catalysts

Catalysts	BET surface area / m^2 g^{-1}		Rh dispersion[a] (%)	
	Fresh	Aged[b]	Fresh	Aged[b]
Rh/ZrO_2	52.3	16.4	54.9	6.5
Rh/Zr–Y–O	57.3	21.4	68.3	5.3
Rh/Zr–La–O	85.8	29.6	87.4	4.5
Rh/Zr–Y–La–O	75.3	51.2	85.2	9.3

[a] Determined by CO chemisorption.

[b] Aged at 1273 K for 24 h in 2 % O_2 and 10 % H_2O/N_2 atmosphere.

3-4. Temperature-programmed reduction by CO (CO-TPR)

Temperature-programmed reduction profiles of the fresh catalysts are presented in Fig. 7. The O/Rh atomic ratios calculated from the TPR data are shown in Table 2. A higher O/Rh ratio (1.48) was measured for fresh Rh/Zr–Y–O compared with Rh/ZrO_2 (0.14). In our previous study, the oxidation state of rhodium on ZrO_2 analyzed by X-ray photoelectron spectroscopy (XPS) was trivalent after being oxidized by 5 % O_2. The difference between the low O/Rh ratio for Rh/ZrO_2 and the presence of trivalent rhodium from XPS results indicated that only the surface of rhodium particles were oxidized to Rh^{3+}.[22] Conversely, the O/Rh ratio was 1.48 for Rh/Zr–Y–O, indicating that all the rhodium particles were almost fully oxidized. Similarly, the amount of CO_2 generated during the TPR process increased by the addition of Y to Rh/Zr–La–O (Fig. 7c and d). A larger O/Rh ratio of 1.20 was measured for Rh/Zr–Y–La–O, while Rh/Zr–La–O had a lower O/Rh ratio of 0.70. The TPR profile also changed by Y addition to Rh/Zr–La–O. It should be noted that Rh/Zr–Y–La–O was more readily reduced at low temperature than Rh/Zr–La–O (Fig. 7c and d). These results indicate, for the fresh catalysts, that Y addition caused Rh to be more readily oxidized and the reducibility of Rh was also enhanced by the addition of Y to the La-containing catalyst. Figure 8 presents the CO-TPR profiles of the aged catalysts. A sharp peak was observed at 520 K for Rh/ZrO_2 and Rh/Zr–Y–O, as shown in Fig. 8a and b, respectively. Conversely, the aged Rh/Zr–La–O and Rh/Zr–Y–La–O catalysts exhibited a broad reduction profile starting at around 500 K (Fig. 8c and d). No significant effect of Y addition on the reduction profiles was detected for the aged catalysts.

Table 2 Amount of CO_2 (μmol g^{-1}) released during CO-TPR and O/Rh ratios

Catalysts	Amount of CO_2 released / μmol g^{-1}		O/Rh ratio[a]	
	Fresh	Aged[b]	Fresh	Aged[b]
Rh/ZrO_2	45	59	0.14	0.20
Rh/Zr–Y–O	428	36	1.48	0.12
Rh/Zr–La–O	224	121	0.70	0.42
Rh/Zr–Y–La–O	344	155	1.20	0.54

[a] Determined by CO-TPR.

[b] Aged at 1273 K for 24 h in 2 % O_2 and 10 % H_2O/N_2 atmosphere.

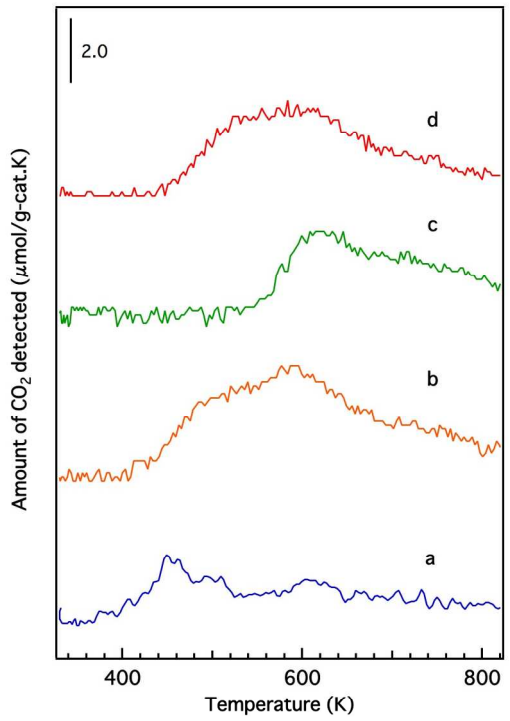

Fig. 7. CO-TPR profiles of the fresh catalysts: (a) Rh/ZrO_2, (b) Rh/Zr–Y–O, (c) Rh/Zr–La–O and (d) Rh/Zr–Y–La–O.

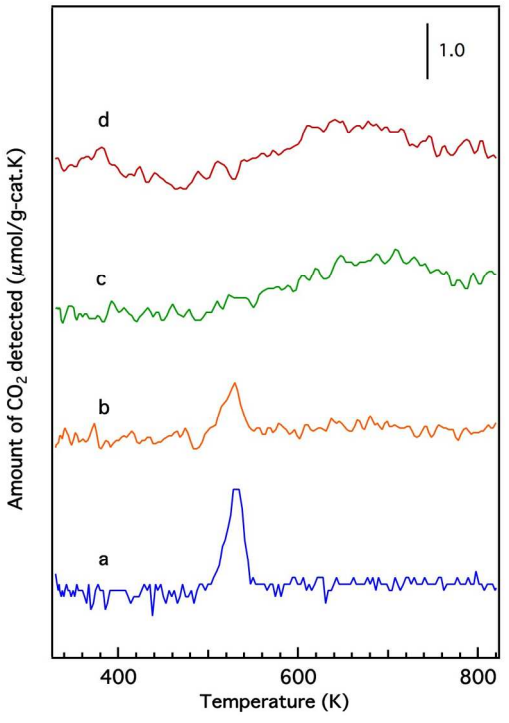

Fig. 8. CO-TPR profiles of the aged catalysts: (a) Rh/ZrO_2, (b) Rh/Zr–Y–O, (c) Rh/Zr–La–O and (d) Rh/Zr–Y–La–O.

3-5. Infrared spectra

Although XPS is a powerful tool to investigate the oxidation state of rhodium, the Y $3p_{3/2}$ signal at 311 eV overlaps with the Rh $3d_{5/2}$ signal at 307 eV. Therefore, in the case of Y-containing materials, information about rhodium was not accessible, especially when the loading of rhodium was as low as 0.33 wt %, as was the case in this study. For this reason, we employed NO molecules as probes for the Rh metallic state because it is widely accepted that NO readily forms Rh^0-NO adsorbate on rhodium particles.[24, 25]

Figure 9 presents the IR absorption spectra of the Rh/Zr–La–O and Rh/Zr–Y–La–O catalysts after exposure to NO at various temperatures. Several bands associated with NO_x adsorbate were clearly detected for the La-containing catalysts. Bands at 1894, 1857, 1533, 1242 and 1185 cm^{-1} were observed for Rh/Zr–La–O (Fig. 9a). The band at 1857 cm^{-1} was assigned to Rh^0-$NO^{\delta+}$,[24] and the bands from 1533–1185 cm^{-1} were attributed to nitrate species.[26] The band at 1894 cm^{-1} was assigned to Rh^I-NO^+.[27] In the case of Rh/Zr–Y–La–O, the intensity of the Rh^0-NO band at 1848 cm^{-1} was higher than for Rh/Zr–La–O at temperatures from 473–573 K (the magnified bands in Fig. 9). These results indicate that the amount of Rh^0 on the surface was higher for Rh/Zr–Y–La–O than for Rh/Zr–La–O.

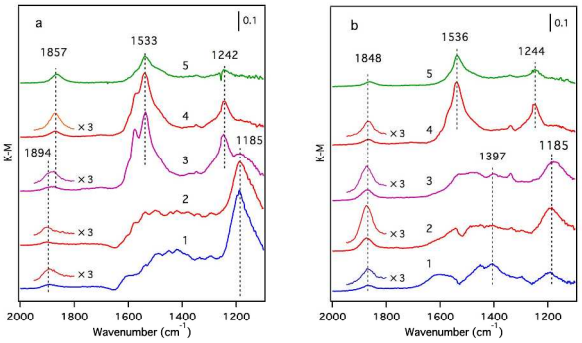

Fig. 9. IR spectra of NO absorbed on fresh (a) Rh/Zr–La–O, (b) Rh/Zr–Y–La–O. Spectra were taken at (1) 373 K, (2) 473 K, (3) 573 K, (4) 673 K and (5) 773 K.

3-6. Steam reforming reaction activity and its effect on three-way catalysis

The steam reforming reaction is influential in three-way catalysis for enhancing NO_x conversion by producing hydrogen as a reductant. This reaction is known to proceed over Rh catalysts.[28, 29] Previously, we reported that exposure to the steam reforming reaction reduced the oxidized rhodium and recovered the activity of the catalyst.[22] In this study, the effect of Y addition on this reaction was examined. Figure 10 presents C_3H_6 conversion in the steam reforming reaction over the fresh catalysts. The addition of Y to ZrO_2 resulted in a dramatic decrease in the activity of this reaction. Yttrium addition to La-containing ZrO_2 decreased the activity by a small amount, but

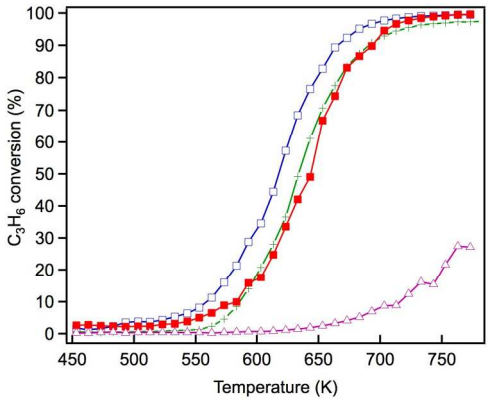

Fig. 10. C_3H_6 conversion in the steam reforming reaction over the fresh Rh catalysts: (+) Rh/ZrO_2, (△) Rh/Zr–Y–O, (□) Rh/Zr–La–O and (■) Rh/Zr–La–Y–O.

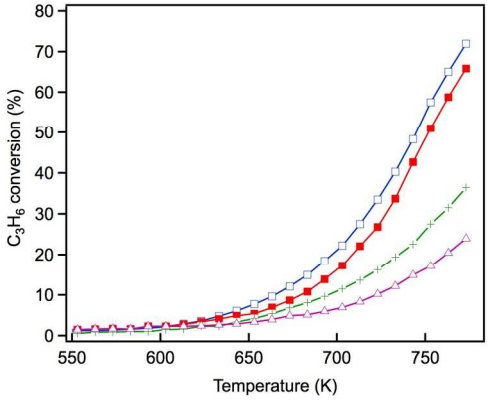

Fig. 11. C_3H_6 conversion in the steam reforming reaction over the aged Rh catalysts: (+) Rh/ZrO_2, (△) Rh/Zr–Y–O, (□) Rh/Zr–La–O and (■) Rh/Zr–La–Y–O.

the catalyst still maintained high activity. Figure 11 presents C_3H_6 conversion in the steam reforming reaction over the aged catalysts. Both Rh/Zr–La–O and Rh/Zr–Y–La–O exhibited superior activity compared with Rh/ZrO_2 and Rh/Zr–Y–O. It is evident that when Y was added to the support, the presence of La was highly effective in maintaining the catalyst's high steam reforming reaction activity for both fresh and aged catalysts.

The influence of the steam reforming reaction on the activity of the three-way catalysis was investigated for Rh/Zr–Y–O and Rh/Zr–Y–La–O to identify the impact of Y addition on the reaction. Figure 12a and b present the results for the aged Rh/Zr–Y–O and Rh/Zr–Y–La–O, respectively. First, the three-way catalytic activity of the aged catalysts was examined without any pre-treatment (curve 1 in each figure). The next experiments examined the three-way catalysis of the aged catalysts after pre-treatment under a 5 % O_2 flow at 773 K for 5 min (curves 2 in each figure). The final experiments investigated the three-way catalytic activity of the aged catalysts that were oxidized under a 5 % O_2 flow at 773 K for 5 min followed by the steam reforming reaction at 520 K for 5

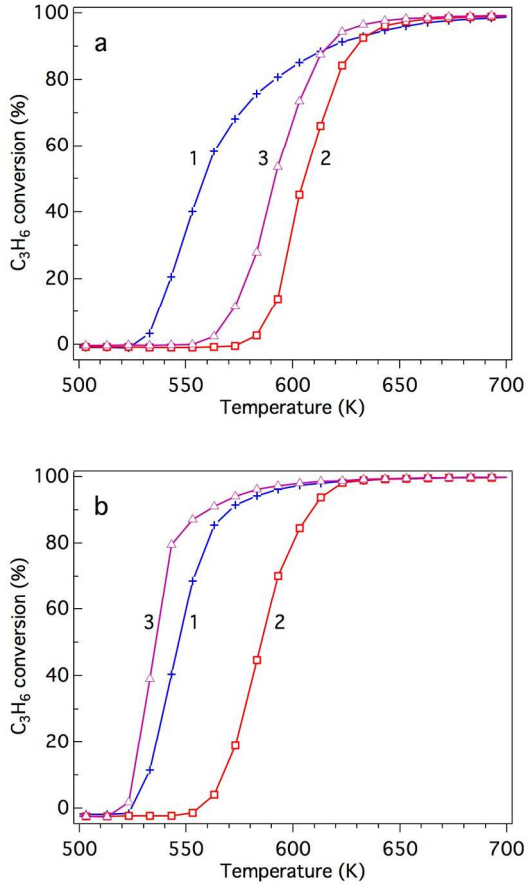

Fig. 12. Effect of the steam reforming reaction for the three-way catalytic C_3H_6 conversion by the (a) aged Rh/Zr–Y–O and (b) aged Rh/Zr–Y–La–O catalysts. Three types of pre-treatment were conducted: (1) no pre-treatment, (2) pre-treatment with 5 % oxygen at 773 K for 5 min, and (3) pre-treated with 5 % oxygen at 773 K for 5 min followed by the steam reforming reaction at 520 K for 5 min.

min (curves 3 in each figure). The oxidative pre-treatment caused dramatic decreases in the three-way catalytic activities for the two tested catalysts. In the case of Rh/Zr–Y–O, which had low steam reforming activity, recovery of the three-way catalytic activity after the steam reforming reaction was limited (Fig. 12 a, curve 3). Conversely, Rh/Zr–Y–La–O showed a complete recovery (Fig. 12 b, curve 3) after the steam reforming reaction from the low activity after the oxidation treatment (Fig. 12 b, curve 2). Besides hydrogen and CO generated by the steam reforming reaction, C_3H_6 also recovered the three-way catalytic activity for Rh/Zr–La–O (results not shown). Recovery of the catalyst by the steam reforming reaction included the contribution of C_3H_6 as a reductant. These experiments demonstrated that the regenerative effect of the steam reforming reaction worked well for Rh/Zr–Y–La–O, as was also observed for Rh/Zr–La–O in our previous study.[21]

4. Discussion

We have previously reported that rhodium supported on Zr–La–O was highly active under fresh and the aged conditions.[22] Rhodium supported on Zr–La–O maintained its low oxidation state during the three-way catalytic reaction and after the oxidative treatment. This performance was not achieved when other lanthanides (Ce, Pr, or Nd) were added to the zirconia supports. After the aging treatment, the Rh/Zr–La–O catalyst exhibited higher activity in the steam reforming reaction. It was confirmed that the catalytic activity was recovered because oxidized rhodium was reduced by the steam reforming reaction. The aging treatment transformed the structure of the Zr–La–O support from tetragonal to three phases: monoclinic-ZrO_2, tetragonal-ZrO_2 and pyrochlore ($La_2Zr_2O_7$). The treatment also altered the rhodium particle size from a few nanometers to 30–100 nm. In this study, Y was added to the ZrO_2-based supports to stabilize the structure and its effect was investigated based on the state of Rh, activity for the steam reforming reaction and the three-way catalytic performance. As a result, it was found that Rh/Zr–Y–La–O showed excellent three-way catalytic performance that was better than a previously reported Rh/Zr–La–O catalyst.[21, 22]

For the fresh Rh/ZrO_2 and Rh/Zr–Y–O catalysts, Y addition to ZrO_2 enhanced the oxidation of Rh, as demonstrated by the results of O/Rh ratio derived from CO-TPR. The O/Rh ratio increased from 0.14 for Rh/ZrO_2 to 1.48 for Rh/Zr–Y–O (Table 2). The O/Rh ratio of 1.48 for Rh/Zr–Y–O was almost the stoichiometric value corresponding to the formation of fully oxidized Rh_2O_3 particles. Also, the introduction of Y induced a dramatic decrease in the steam reforming activity of the fresh catalysts (Fig. 10). As a result, the three-way catalytic activity of Rh/Zr–Y–O was low. The oxidation states of Rh for the two aged catalysts were similar to each other; the O/Rh ratios for Rh/ZrO_2 and Rh/Zr–Y–O were 0.20 and 0.12, respectively. The sharp TPR peaks (Fig. 8 a and b) suggest that only the surfaces of rhodium particles were oxidized to Rh_2O_3 in each aged sample. The steam reforming activities were very low for the aged catalysts. In particular, Rh/Zr–Y–O had the lowest activity (Fig. 11). The limited regeneration was demonstrated for the aged Rh/Zr–Y–O catalyst, as shown in Fig. 12 a. The lower three-way catalytic activities of these two catalysts can be readily explained by their low regeneration. The reason why the aged Rh/Zr–Y–O showed three-way catalytic activity higher than the aged Rh/ZrO_2 is unclear.

The enhancement of rhodium oxidation by Y addition was also observed for fresh Rh/Zr–Y–La–O. Also, the introduction of Y to Zr–La–O improved the reducibility of rhodium oxides (lower reduction temperature at CO-TPR). Enhancement of rhodium oxidation was indicated by the increased O/Rh ratio from 0.70 for Rh/Zr–La–O to 1.20 for Rh/Zr–Y–La–O (Table 2). In our previous report,[22] the oxidation state of rhodium on Zr–La–O after oxidative pre-treatment averaged between Rh^0 and Rh^{3+} (Fig. S9 in the ESI). These results indicate that rhodium particles became more readily oxidized after Y addition. The CO-TPR profile of the fresh Rh/Zr–Y–La–O showed that

rhodium on Zr–Y–La–O was more readily reduced than that on Zr–La–O. Specifically, the reduction profile of Rh/Zr–La–O began at approximately 540 K, but in the case of Rh/Zr–Y–La–O, the profile started from a much lower temperature (440 K, Fig. 7c and d). IR spectra of adsorbed NO also revealed that the band assigned to Rh^0-NO^+ was enhanced by Y addition, especially at around 473 K, the temperature at which the three-way catalytic reaction started (Fig. 9b). This is also an indication of the presence of rhodium (0) on the surface, highlighting that the rhodium on Zr–Y–La–O was reduced more readily than on Rh/Zr–La–O. Also, Rh/Zr–Y–La–O demonstrated a high steam reforming activity that was comparable to Rh/Zr–La–O (Fig. 10). Therefore, the regeneration of Rh was likely pronounced during the three-way catalysis over Rh/Zr–Y–La–O.

Y addition did not affect rhodium oxidation for the aged catalysts as indicated by the results of the CO-TPR profiles (Fig. 8). Aged catalysts contain larger Rh particles as was indicated by their low Rh dispersion. Thus, it is unlikely that the oxide support influences the oxidation of rhodium through interactions between the Rh particles and the support. The XRD results for Rh/Zr–Y–La–O after the aging treatment showed that Y addition prevented phase separation (Fig. 1h). Stabilization of the support was also reflected in the changes of BET surface areas before and after the aging treatment. Rh/Zr–La–O decreased its surface area to 29.6 m^2g^{-1}, while Rh/Zr–Y–La–O had a surface area as high as 51.2 m^2g^{-1}. The relatively high rhodium dispersion for the aged Rh/Zr–Y–La–O (Table 1) was likely from the high surface area of the support after the aging treatment. The small rhodium particles in the TEM images correlated well with the dispersion for aged Rh/Zr–Y–La–O (Fig. 6). The high steam reforming activity was maintained, even after Y addition (Fig. 11). It was also confirmed that the steam reforming reaction recovered the catalytic activity that was deactivated by the oxidative treatment (Fig. 12 b).

Steam-reforming reaction is endothermic reaction.[32] The fact that the outlet temperature was lower compared to the inlet temperature during three-way catalysis above 673 K demonstrated that the endothermic reaction was taking place during the three-way catalysis (Fig. S6 in ESI). Rh/Zr–Y–La–O showed high steam-reforming activity (Fig. 11), and correspondingly the recovery of the catalyst was confirmed. (Fig. 12b). Based on these findings, it is reasonable to conclude that the recovery of the catalyst by the steam-reforming reaction was taking place under the actual three-way catalysis conditions. Therefore, the recovery function of Rh/Zr–Y–La–O can be regarded as "self-regeneration". Overall, Rh/Zr–Y–La–O showed excellent performance, even after the aging treatment.

5. Conclusions

High activity for fresh and aged Rh/Zr–Y–La–O in three-way catalytic processes was identified in this study. The effects of Y addition to the supports were also investigated in detail. Yttrium addition to Rh/Zr–La–O increased the oxidation of rhodium compared with Rh/Zr–La–O, but the reducibility of rhodium was also enhanced, as indicated by CO-TPR. Rh/Zr–Y–La–O showed high steam reforming activity, comparable to Rh/Zr–La–O. Thus, the regeneration of Rh was likely pronounced for Rh/Zr–Y–La–O. In the case of Rh/Zr–Y–O, rhodium particles were fully oxidized after an oxidation treatment. Yttrium addition to ZrO_2 dramatically decreased the steam reforming activity. Rhodium particles on ZrO_2 and Zr–Y–O are readily oxidized during reaction, leading to low three-way catalytic activity.

After the aging treatment, Rh/Zr–Y–La–O showed higher rhodium dispersion than the other tested catalysts. This is likely because of the relatively high surface area of the support after the aging treatment and stabilization of ZrO_2 by the addition of Y. Excellent steam reforming activity was maintained for Rh/Zr–Y–La–O after the aging treatment. The high steam reforming activity regenerates deactivated oxidized Rh, providing the best three-way catalytic activity. These results demonstrate the importance of the catalyst support in designing three-way catalysts. Our findings highlight the potential to design and develop effective three-way catalysts with high tolerances to oxidative reaction conditions in recently developed vehicles and engines.

Notes and references

[a] Advanced Materials Research Field, Technical Research Center, Mazda Motor Corporation, 3-1 Shinchi, Fuchu-cho, Aki-gun, Hiroshima 730-8670, Japan. E-mail: kawabata.h@mazda.co.jp; Fax: +81-82-252-5342; Tel: +81-82-252-5068

[b] Department of Applied Chemistry, Graduate School of Engineering, Hiroshima University, 1-4-1 Kagamiyama, Higashi-Hiroshima 739-8527, Japan. E-mail: inumaru@hiroshima-u.ac.jp; Fax: +81-82-424-5494; Tel: +81-82-424-7741

† Electronic Supplementary Information (ESI) available: CO conversion, EDX analysis data, XRD patterns of Rh111 diffraction and XPS spectra are provided. See DOI: 10.1039/b000000x/

1. H. Shinjoh, M. Hatanaka, Y. Nagai, T. Tanabe, N. Takahashi, T. Yoshida and Y. Miyake, Top. Catal, 2009, 52, 1967.
2. J. R. Theis and R. W. McCabe, Catal. Today, 2012, 184, 262.
3. R. Burch, P. K. Loader and N. A. Cruise, Appl. Catal. A, 1996, 147, 375.
4. K. Dohmae, Y. Nagai, T. Tanabe, A. Suzuki, Y. Inada and M. Nomura, Surf. Inter. Anal., 2008, 40, 1751.
5. C. P. Hwang, C. T. Yeh and Q. M. Zhu, Catal. Today, 1999, 51, 93.
6. M. Zimowska, J. B. Wagner, J. Dziedzic, J. Camra, B. Borzeccka-Prokop and M. Najbar, Chem. Phys. Lett., 2006, 417, 137.
7. R. W. McCabe, R. K. Usmen, K. Ober and H. S. Gandhi, J. Catal., 1995, 151, 385.
8. M. Uenishi, H. Tanaka, M. Taniguchi, I. Tan, Y. Nishihata, J. i. Mizuki and T. Kobayashi, Catal. Commun., 2008, 9, 311.
9. S. I. Matsumoto, Catal. Today, 2004, 90, 183.
10. H. Muraki and G. Zhang, Catal. Today, 2000, 63, 337.
11. H. S. Gandhi, G. W. Graham and R. W. McCabe, J.Catal., 2003, 216, 433.
12. M. Shelef and R. W. McCabe, Catal. Today, 2000, 62, 35.

13. G. C. Koltsakis and A. M. Stamatelos, Prog. Ener. Comb. Sci. 1997, 23, 1.
14. M. Shelef and G. W. Graham, Catal. Rev. Sci. Eng., 1994, 36, 433.
15. Z. WengSieh, R. Gronsky and A. T. Bell, J.Catal., 1997, 170, 62.
16. D. J. C. Yates and E. B. Prestridge, J.Catal, 1987, 106, 549.
17. M. A. Newton, Chem. Soc. Rev., 2008, 37, 2644.
18. M. A. Newton, B. Jyoti, A. J. Dent, S. G. Fiddy and J. Evans, Chem. Commun., 2004, 2382.
19. T. Tanabe, A. Morikawa, M. Hatanaka, N. Takahashi, Y. Nagai, A. Sato, O. Kuno, H. Suzuki and H. Shinjoh, Catal. Today, 2012, 184, 219.
20. R. Burch and P. K. Loader, Appl. Catal. A, 1996, 143, 317.
21. H. Kawabata, Y. Koda, H. Sumida, M. Shigetsu, A. Takami and K. Inumaru, Chem. Commun., 2013, 49, 4015.
22. H. Kawabata, Y. Koda, H. Sumida, M. Shigetsu, A. Takami and K. Inumaru, Catal. Sci. Tech., 2014, 4, 697.
23. H. G. Scott, J.Mater. Sci, 1975, 10, 1527.
24. C. Dujardin, A. S. Mamede, E. Payen, B. Sombret, J. P. Huvenne and P. Granger, Top. Catal., 2004, 30-1, 347.
25. T. Chafik, A. M. Efstathiou and X. E. Verykios, J. Phys. Chem. B, 1997, 101, 7968.
26. M. Haneda, K. Shinoda, A. Nagane, O. Houshito, H. Takagi, Y. Nakahara, K. Hiroe, T. Fujitani and H. Hamada, J. Catal., 2008, 259, 223.
27. E. Rogemond, N. Essayem, R. Frety, V. Perrichon, M. Primet, M. Chevrier, C. Gauthier and F. Mathis, J. Catal., 1999, 186, 414.
28. J. Barbier-Jr and D. Duprez, Appl. Catal. B, 1994, 4, 105.
29. J. P. Breen, R. Burch and H. M. Coleman, Appl. Catal. B, 2002, 39, 65.
30. J. A. Anderson, M. Fernandez Garcia (Eds.), Supported Metals in Catalysis, ICP, London, 2005, p.140.
31. "Shokubai-kouza", vol. 5, Catalyst design, ISBN: 4061914057, Kodan-sha, 1985, p.141.
32. M. E. Domine, E. E. Iojoiu, T. Davidian, N. Guilhaume and C. Mirodatos, Catal. Today, 2008, 133, 565.

" Highly active three-way catalysis of rhodium particles on a Y-stabilized La-containing ZrO_2 support: Effect of Y on the enhanced reducibility of rhodium and self-regeneration" by H. Kawabata, Y. Koda, H. Sumida, M. Shigetsu, A. Takami and K. Inumaru (Corresponding author: H. Kawabata).

Contents entry:

A novel, highly active three-way catalyst, rhodium supported on Y- and La-added zirconia (Rh/Zr–Y–La–O) was found in this study.

Graphical abstract: